Available online at www.sciencedirect.com
SCIENCE DIRECT
Journal of African Earth Sciences 44 (2006) 331–338
Journal of African Earth Sciences
www.elsevier.com/locate/jafrearsci

The structure of a Mesozoic basin beneath the Lake Tana area, Ethiopia, revealed by magnetotelluric imaging

Sophie Hautot [a,*], Kathryn Whaler [a], Workneh Gebru [b], Mohammednur Desissa [c]

[a] School of GeoSciences, The University of Edinburgh, West Main Road, EH3 9JW Edinburgh, UK
[b] Petroleum Operations Department, Ministry of Mines, Addis Ababa, Ethiopia
[c] Geological Survey of Ethiopia, Addis Ababa, Ethiopia

Received 18 April 2005; received in revised form 21 October 2005; accepted 16 November 2005
Available online 27 January 2006

Abstract

The northwestern Plateau of Ethiopia is almost entirely covered with extensive Tertiary continental flood basalts that mask the underlying formations. Mesozoic and Tertiary sediments are exposed in a few locations surrounding the Lake Tana area suggesting that the Tana depression is an extensional basin buried by the 1–2 km thick Eocene–Oligocene flood basalt sequences in this region. A magnetotelluric survey has been carried out to investigate the deep structure of the Tana area. The objectives were to estimate the thickness of the volcanics and anticipated underlying sedimentary basin. We have collected 27 magnetotelluric soundings south and east of Lake Tana. Two-dimensional inversion of the data along a 160 km long profile gives a model consistent with a NW–SE trending sedimentary basin beneath the lava flows. The thickness of sediments overlying the Precambrian basement averages 1.5–2 km, which is comparable to the Blue Nile stratigraphic section, south of the area. A 1 km thickening of sediments over a 30–40 km wide section suggests that the form of the basin is a half-graben. It is suggested that electrically resistive features in the model are related to volcanic materials intruded within the rift basin sediments through normal faults. The results illustrate the strong control of the Precambrian fracture zones on the feeding of the Tertiary Trap series.

Keywords: Ethiopia; Magnetotellurics; Mesozoic sediments; Flood basalts

1. Introduction

In Ethiopia, Mesozoic and/or Tertiary sediments are exposed in the south-eastern plateau, in the Ogaden rift (Fig. 1(a)). In the northwestern plateau, they are exposed in Mekele, Metema, and the Blue Nile river basin (Fig. 1(a)). Elsewhere the subsurface structure is poorly known because the plateau is covered with a large volume of volcanic materials erupted between ~40 and 22 Ma, with a clear pulse between 31 and 29 Ma (Hofmann et al., 1997; Kieffer et al., 2004).

The Tana basin, northwest Ethiopia is an uplifted dome possibly related to the Afar mantle plume (Pik et al., 2003). The basin was formed by faulting of mid-Tertiary basalts. The Tertiary basalt cover in the Tana area is assumed to average 500–1500 m in thickness (Jepsen and Athearn, 1961; Pik et al., 2003). It was suggested from digital elevation modelling and satellite imagery analysis that Lake Tana occupies a centre of subsidence and convergence of three grabens (Chorowicz et al., 1998). Our area of study is south and east of the lake Tana, in the ESE-WNW Debre Tabor graben (Chorowicz et al., 1998).

Without any information on the structure of the Tana region beneath the volcanic series, the relationships between the location of the eruption of the continental flood basalts and weakness zones in the crust cannot be confirmed. However, one preferential orientation of the

* Corresponding author. Present address. IUEM-UBO, UMR CNRS 6538 "Domaines Océaniques", Place Nicolas Copernic, 29280 Plouzané, France. Tel.: +33 298 498 748; fax: +33 298 498 760.
E-mail address: hautot@univ-brest.fr (S. Hautot).

1464-343X/$ - see front matter © 2005 Elsevier Ltd. All rights reserved.
doi:10.1016/j.jafrearsci.2005.11.027

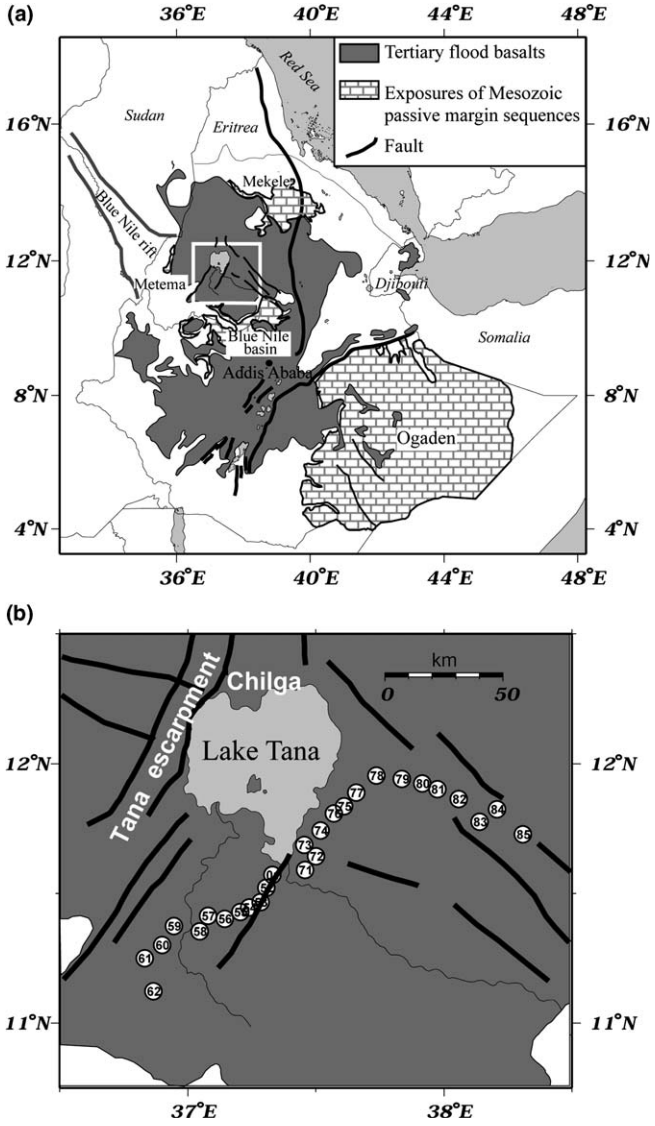

Fig. 1. (a) Simplified geological map of Ethiopia. Modified after Tadesse et al. (2003) and Mège and Korme (2004). The white square shows the Tana area. (b) Location map of the Tana area corresponding to the white square in (a). The numbered circles show the location of the magnetotelluric soundings. Colors and symbols for the geology are the same as in (a) (For interpretation of the references in colour in this figure legend, the reader is referred to the web version of this article).

dyke swarms feeding the northwestern volcanic plateau in the Tana area has been related to the NW–SE trending Precambrian fracture zone (Mège and Korme, 2004). The NW–SE Precambrian fracture zone was reactivated south of the Tana region during the Late Paleozoic–Mesozoic with the extension of the Ogaden rift. In southern and eastern Sudan and in Kenya, NW–SE trending Mesozoic and Tertiary sedimentary basins are related to failed phases of continental rifting associated with the Central African Rift system (Bosworth, 1992; Morley et al., 1999; Ebinger et al., 2000).

The Tana basin is aligned with two NW–SE structures of different ages: the Late Jurassic–Cretaceous Blue Nile rift, south Sudan, and the Late Paleozoic–Mesozoic Ogaden rift (Fig. 1(a)). Mesozoic and/or Tertiary sediments are exposed south (Blue Nile Basin), East (Mekele Basin), and West (Metema Basin) of Lake Tana (Getaneh, 1991) suggesting the existence of sediments in the Tana region (Fig. 1(a)) although this assumes a correlation over long distances. More constrained information is given by the presence of marine Mesozoic strata, 200 m thick, that are exposed on the Tana escarpment (Fig. 1(b)), west of the lake (Chorowicz et al., 1998) and the marine Mesozoic sequence that totals 880 m, in the Blue Nile Basin, to the south (Getaneh, 1991). North of the lake, at least 130 m of Oligocene fluvial sediments were deposited in the Chilga basin (Fig. 1(b)), the southern part of the NS trending Gondar graben, formed by faulting of ~30 Ma basalts (Kappelman et al., 2003). From stratigraphic sections constructed at different places along the Blue Nile River, the presence of clastic, carbonate and evaporitic sediments indicate that this passive continental margin has undergone marine transgression and regression (Wolela, 1997). The marine sequence of the Blue Nile basin may be underlain by rift basins that are believed to be an extension of the NW–SE trending Karroo rift system of the Ogaden Basin, known for its potential for oil and gas (Tadesse et al., 2003). The structural evolution and stratigraphic units encountered in the Blue Nile basin are broadly equivalent to those of the Ogaden (Worku and Askin, 1992), which suggests that the basin might have similar hydrocarbon potential.

This paper describes how magnetotelluric data have been used to investigate the existence and thickness of sub-basalt sedimentary basins in the Lake Tana region (Fig. 1(a) and (b)). Magnetotelluric (MT) imaging is appropriate to characterize sedimentary structure beneath the lava flows because electrically resistive volcanics do not mask the more conductive underlying formations. A MT profile was acquired south and east of the lake (Fig. 1(b)) to provide a resistivity model of the subsurface down to the Precambrian basement. The MT modelling results show a high resistivity contrast between the different geological formations that allows the geometry of the structures beneath the basaltic layers and above the basement to be constrained. The results are consistent with a NW–SE orientated sedimentary basin beneath the lava flows.

2. Magnetotelluric data acquisition and processing

We carried out 27 MT soundings along a 220 km long profile (Fig. 1(b)) with the SPAM data acquisition system (Ritter et al., 1998). The horizontal electric and magnetic field time series were recorded in the 1/128–2048 s period band in the magnetic north (x) and east (y) directions. The electric potentials were measured between two non-polarizable Cl_2–$PbCl_2$ electrodes, with separations of 30–55 m. A 150 km section of the profile is oriented NE-SW, perpendicular to the strike of the main faults. The eastern part is roughly WNW–ESE, due to limited

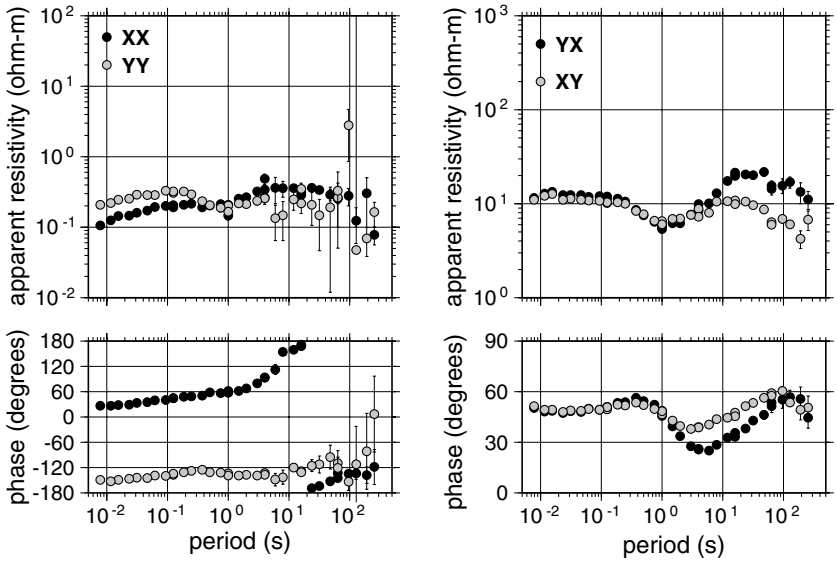

Fig. 2. Example of the magnetotelluric impedance tensor. The four complex elements, Z_{xx} and Z_{yy} (left) and Z_{xy} and Z_{yx} (right) of the impedance tensor at site 61 are shown in terms of apparent resistivity and phase. The error bars are one standard deviation.

road access to the north (Fig. 1(b)). The station spacing varies between 5 and 10 km.

The electric and magnetic field time series were transformed into the frequency domain. The 2×2 MT impedance tensor $\mathbf{Z}$ relating the horizontal electric (E_x, E_y) to the horizontal magnetic (B_x, B_y) fields was determined using the robust remote reference method of Chave and Thompson (1989). At most of the sites, we obtained good data quality in the period range 1/128–256 s allowing several kilometres penetration depth. An example of MT impedance (site 61) representative of the whole data set is presented in Fig. 2. Both the amplitudes (expressed in apparent resistivity units, Ω-m) and phases of the off diagonal (xy and yx) and the diagonal (xx and yy) terms are shown.

In a 2-D Earth, the electromagnetic induction equations separate into two modes, the transverse electric (TE) mode (currents parallel to structure and in the direction of constant conductivity, the geoelectrical strike) and the transverse magnetic (TM) mode (currents perpendicular to geoelectrical strike). Currents parallel to structure only induce magnetic fields perpendicular to it, and vice versa for the TM mode. Thus the diagonal elements of the impedance tensor vanish. The MT impedance tensor at each site was rotated to the direction that best-fits an off-diagonal tensor. The geoelectrical strike direction was determined by rotating the impedance tensor into the complex direction minimizing its diagonal elements. This was done choosing the rotation angle of the real axis of the electric or magnetic field that either maximizes or minimizes the impedance tensor. This angle defines, for each period, a maximum electric field direction (MED) or a minimum magnetic field direction (Counil et al., 1986). In a 2-D geometry the MED corresponds to the strike of the 2-D structure. At most sites, the rotation angle was well defined and constant with period, although the direction changes at periods >10–20 s at others indicate a structural direction change at greater depths. This is illustrated in Fig. 3 where the MED are shown for period of 0.5 and 48 s. At 0.5 s period, representative of approximately the first kilometre below surface, there are two main directions, 110–150°N and 20–60°N, that agree well with the two Pan-African basement fracture and shear zone trends in NE Africa (Abdelsalam and Stern, 1996). The 110–150°N direction corresponds to the NW–SE direction of the Mesozoic-Early Tertiary basins in South Sudan (Bosworth, 1992) while the 20–60° direction corresponds to the NNE–SW Pan-African basement shear zone trend. At longer periods (48 s on Fig. 3), the NW–SE direction clearly dominates, indicating that deeper structures are more influenced by the fault direction that was reactivated during rifting. Twenty-one sites along a NE–SW profile (from 79 in the NE to 62 in the SW) were considered for modelling in order to investigate the deep structure of the main NW–SE geological trend.

3. Modelling

The 2-D inversion method used is based on an iterative technique that minimizes a misfit function between the data and the 2-D model calculation in both TE and TM modes (Hautot et al., 2002). The forward problem is solved with a finite-difference 2-D algorithm. The 2-D model space is parameterized by blocks of uniform resistivity whose thickness increases with depth.

For each site, the MED was compared to the main tectonic trend to determine which of the maximum or minimum components corresponds to the TE mode (and, respectively, to the TM mode). The 2-D model overlies a homogeneous half-space and sits between two 1-D

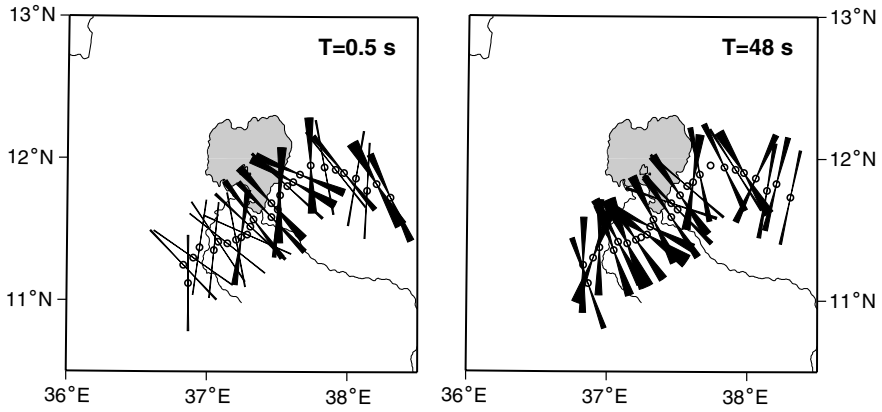

Fig. 3. Maximum electrical field direction (MED) at each site at the period $T = 0.5$ s (left) and 48 s (right). The width of the pie wedge is two standard deviations.

structures to apply the boundary conditions on the calculation. The thickness of the 2-D region was set to 15 km. The parameters of the inversion are the resistivities of each block, the half-space and the 1-D layers. A thin 30 m top layer was added to correct for most of the static shift (Jones, 1988). This was not enough to correct for strong local distortion of the electric field observed at sites 52–73. For these sites, we first minimized the misfit for the full TM impedance and the phase of the TE impedance. We obtain a real static shift factor that was subsequently considered for the inversion of both full TE and TM impedances.

The root-mean-squared (rms) misfit error for the best-fitting 2-D resistivity model is 3. The 2-D MT response of the 2-D model matches the data reasonably well. Six examples are shown in Fig. 4. The best-fitting model is shown in Fig. 5. Although data provide constraints to ~15 km depth, only the upper 5 km of structure is shown because the purpose of this paper is to discuss structures above the basement. The electrical resistivity of rocks depends mainly on the conductive phase (fluids, highly conductive minerals). Sediments are more electrically conductive than unaltered igneous (>1000 Ωm) and volcanic (>few hundred Ωm) rocks. In our model, the resistivity distribution in the top 2–3 km is heterogeneous. There are two well-resolved resistive structures along the profile beneath sites 60–57 and beneath sites 71–73 (labelled R1 and R2 in Fig. 5). These two bodies are in a less resistive medium, which shows a layered structure with an inserted conductive layer (X, Fig. 5), particularly at the two ends of the profile (beneath sites 62–61 and sites 76–79). Below 2–3 km depth, the resistivity is uniformly higher suggesting that the Precambrian basement (B, Fig. 5) has been reached. The top of the basement deepens between sites 59 and 71, down to 5 km depth below surface.

4. Discussion

The observed geoelectric strikes are well correlated to the two main regional tectonic trends identified in the area from surface geology and satellite image analysis (Chorowicz et al., 1998; Mège and Korme, 2004), NW–SE for the main direction and NNE-SSW for local and superficial structures. In the model shown in Fig. 5, the conductive medium (resistivity <20 Ωm) above the basement (B, Fig. 5) can be interpreted as sediments to be correlated with any or all of the Late Paleozoic–Tertiary sediments that were deposited in Ethiopia. Without well data, we cannot make long distance correlations with passive margins sequences in eastern Ethiopia and Somalia or rift sequences in Sudan and northern Kenya. However, the resistivity model can be compared to the lithostratigraphic section of the Blue Nile Basin (Wolela, 1997), south of the surveyed area, and to MT experiments in similar environments (Hautot et al., 2000; Whaler and Hautot, 2006).

On the passive margins, the Adigrat sandstone is a well documented fluviatile to nearshore marine formation, deposited on the basement rocks throughout much of East-Africa and the Middle East (Getaneh, 2002). The thickness of Adigrat sandstone is estimated to be ~450 m in the Blue Nile basin and it attains a maximum of 700 m in the Mekele basin (Wolela, 1997; Getaneh, 2002). The age of the formation is controlled by the continental topography and ranges from Late-Paleozoic to early Jurassic (Bosellini et al., 2001). In the early Jurassic, marine transgression from the East resulted in the deposition of a ~900 m marine sequence composed of limestones, sandstones, shale and evaporites (Bosellini et al., 2001). In the Cretaceous, mudstones and sandstones deposited during a regression stage over a thickness of ~550 m, whereas continental rifting, initiated in the Late Jurassic, continued in Sudan, associated with the Central African Shear zone (Bosworth, 1992).

In our model, the thickness of sediments above the basement is 1.5–2 km at the south-west and north-east ends of the profile. This is in good agreement with the Blue Nile stratigraphic section where a maximum sediment thickness of ~2 km is found (Wolela, 1997). The highly conductive layer (X, Fig. 5) inserted between the two slightly more resistive layers can be interpreted as the Jurassic marine

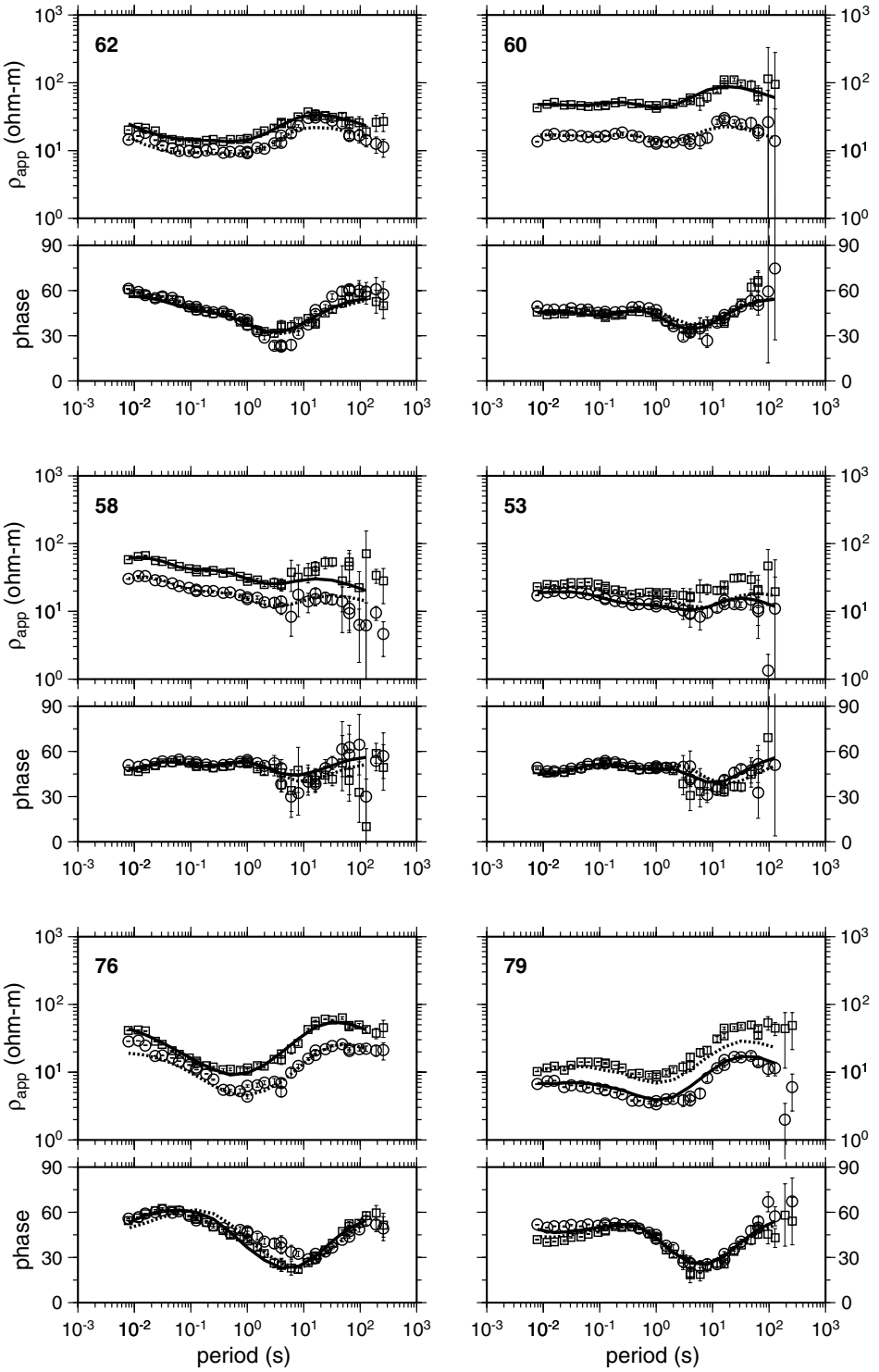

Fig. 4. Examples of the MT data and the fit of the 2-D model shown in Fig. 5. Results are expressed in apparent resistivity units (Ω-m) and phase (degrees). The squares are the components in the maximum impedance direction, and the circles, in the minimum impedance direction. Phases have all been plotted in the first quadrant to show more detail. The dashed line is the TE model response and the solid line the TM model response. The maximum impedance is the TM mode for sites 62, 60, 58, and 76, and the TE mode for sites 53 and 79.

sequence, containing conductive materials such as gypsum and shales. This layer would therefore overly the Adigrat sandstone, deposited on the crystalline basement. Above this possibly Jurassic marine sequence, the age of the formation can range from Late Jurassic to Tertiary. In the Blue Nile gorge section, the Tertiary volcanics lay on 420 m thick sandstone that may have deposited in the Cretaceous (Getaneh, 1991). To the North, in the Chilga basin (Fig. 1(a)), a minimum 130 m thick sequence of lacustrine sediments with an Oligocene date conformably overlays

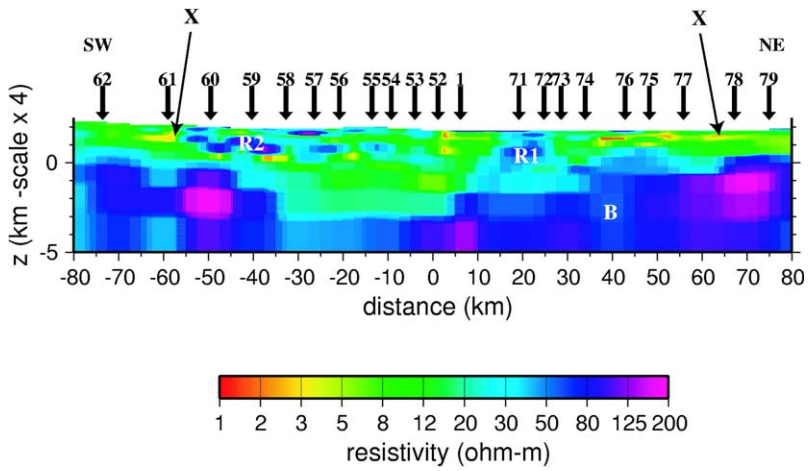

Fig. 5. The 2-D vertical resistivity cross-section from modelling the MT data. The arrows show the locations of the MT sites. X, R1, R2, B: see text for details.

the volcanics (Kappelman et al., 2003). The thickness of the trap series in northwestern Ethiopia averages 1000–1500 m (Pik et al., 2003). In the Blue Nile gorge, Kidane et al. (2002) sampled 230 m thick lava flows. In our model, the thickness of the uppermost resistive layer, which can be interpreted as Tertiary volcanics, does not exceed 250 m (beneath sites 59–55).

Beneath sites 60–73, the structure is more complex than elsewhere along the profile. Two resistive bodies are intruded within the sediments (R1 and R2, Fig. 5) and there is a deepening of the basement top that suggests a 30–40 km wide basin. The resistive bodies (R1 and R2, Fig. 5) intruded in the sedimentary sequence could be associated with volcanic materials. The northwestern Ethiopian Plateau lavas are fissure-fed flood basalts (Pik et al., 1998). A large number of dykes were identified in the Tana area (Chorowicz et al., 1998; Mège and Korme, 2004), and the NW–SE orientation of one of the largest swarms was associated with the NW–SE Precambrian fracture zone reactivated during Mesozoic extension (Mège and Korme, 2004). In the resistivity model shown in Fig. 5, the resistive body (R1, Fig. 5) beneath sites 71–73 extends from surface to the basement along the eastern boundary of the basin structure. We present in Fig. 6 a schematic geological cross-section interpreted from the electrical structure to illustrate the hypothesis that normal faults could have served as fissures feeding the trap series. The second resistive body (R2, Fig. 5), beneath sites 60–62, sits horizontally within the sediments and might be a sill.

The resolution of the resistivity model and lack of nearby information to relate to our structures prevents us dating the tectonic event that resulted in the NW–SE basin between sites 59–71 (Fig. 5). The borders of the basin, interpreted as normal faults as illustrated in Fig. 6, suggests an extensional phase that could be either related to the Late-Paleozoic Early Mesozoic rifting phase or to the Mesozoic Cenozoic Central African rift system, or even both rifting phases. In both cases, continental rifting resulted in NW–SE trending basins, as is the case for the Late Paleozoic–Mesozoic Ogaden rift and for the Mesozoic Tertiary rift in Southern Sudan (Worku and Askin, 1992) and Northern Kenya (Bosworth, 1992). A thickness of 0–350 m Permo-Triassic sediments, underlying the Adigrat sandstones, has been identified in the Blue Nile Basin (Wolela, 1997) and are associated with the Late Paleozoic–Mesozoic rifting phase. The basin could have been reactivated during the

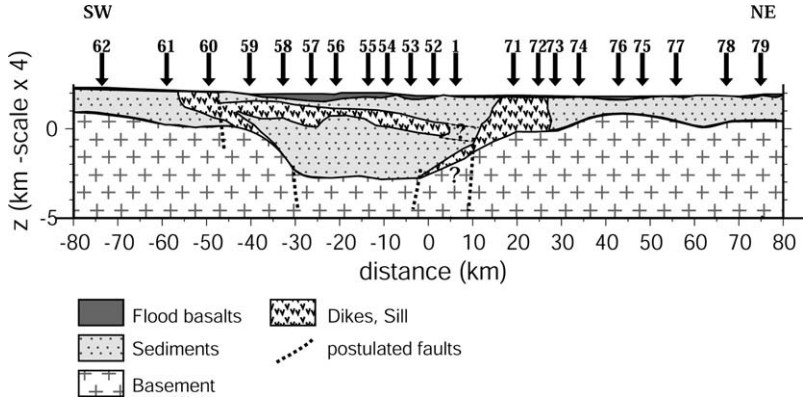

Fig. 6. Schematic geological cross-section interpreted from the resistivity model in Fig. 5. Question marks indicate where it is difficult to distinguish between basement and igneous rocks.

extension phase that occurred during the Mesozoic and early Tertiary in east and central Africa. The width (30–40 km) and thickness (~3 km) of the basin revealed in the resistivity model (Figs. 5 and 6) can be compared to the geometry of the Mesozoic-early Tertiary White Nile and Blue Nile rifts, in south Sudan, with typical widths of 20–50 km and thicknesses of 2.6–3.2 km (Bosworth, 1992).

5. Conclusions

We present the results from a magnetotelluric survey in the Lake Tana region, Ethiopia. The data analysis shows a NW–SE regional geoelectric trend. Two-dimensional modelling of the data was carried out along a NE-SW profile. The model presented is the first geophysical image of the deep structure beneath the Tana region. The electrical structure reveals a 1.5–2 km thick sedimentary series beneath 0–250 m thick continental flood basalts. The sediments could have been deposited from the early Mesozoic to Tertiary. The deepening of the basement over a 30–40 km width is interpreted as the sedimentary infill of a structure inherited from NW–SE Precambrian faults. It is suggested that the continuation from the surface to the basement along the eastern border of the basin of a resistive body is related to dikes that contributed to feed the trap series. The model also provides evidence for sills intruded within the sediments. The intrusion of igneous material within an existing sedimentary basin potentially plays a role in the thermal maturation of the sediments with implications for their resource potential (England et al., 1993).

Acknowledgements

Helpful reviews by two anonymous reviewers are gratefully acknowledged. This work was supported by the Petroleum Operations Department, Ministry of Mines of Ethiopia. It was facilitated by the EAGLE project, especially lead UK participants Peter Maguire and Cindy Ebinger, and NERC grant NER/B/S/2001/00863. SPAM equipment was loaned by the NERC Geophysical Equipment Facility (loan #721), and electrodes by the University of Brest. We are grateful for the assistance and support of field crews. Thanks also to Ahmed Wolela for providing many documents on geology. SH was funded by a Marie Curie Post-Doctoral Fellowship at the University of Edinburgh. Contribution 979 of the IUEM, European Institute for Marine Studies (Brest, France).

References

Abdelsalam, M.G., Stern, R.J., 1996. Sutures and shear zones in the Arabian-Nubian Shield. J. Afr. Earth Sci. 23, 289–310.

Bosellini, A., Russo, A., Assefa, G., 2001. The Mesozoic succession of Dire Dawa, Harar Province, Ethiopia. J. Afr. Earth Sci. 32, 403–417.

Bosworth, W., 1992. Mesozoic and early Tertiary rift tectonics in east Africa. Tectonophysics 209, 115–137.

Chave, A.D., Thompson, D.J., 1989. Some comments on magnetotelluric response function estimation. J. Geophys. Res. 94, 14202–14215.

Chorowicz, J., Collet, B., Bonavia, F.F., Mohr, P., Parrot, J.F., Korme, T., 1998. The Tana basin, Ethiopia: intra-plateau uplift, rifting and subsidence. Tectonophysics 295, 351–367.

Counil, J.-L., Le Mouël, J.-L., Menvielle, M., 1986. Associate and conjugate direction concepts in magnetotellurics. Ann. Geophys. 4, 115–130.

Ebinger, C.J., Yemane, T., Harding, D.J., Tesfaye, S., Kelley, S., Rex, D.C., 2000. Rift deflection, migration, and propagation: linkage of the Ethiopian rift and eastern rifts, Africa. Bull. Geol. Soc. Am. 112, 163–176.

England, R.W., Butler, R.W.H., Hutton, D.H., 1993. The role of Palaeocene magmatism in the Tertiary evolution of basins on the NW seaboard. In: Parker, J.R. (Ed.). Petroleum Geology of Northwest Europe: Proceedings of the 4th Conference. pp. 97–105.

Getaneh, A., 1991. Lithostratigraphy and environment of deposition of Late Triassic to Early Cretaceous sequences of the central part of Northwestern Plateau. Ethiopia. N. Jb. Geol. Palaont. Abb. 182, 255–284.

Getaneh, W., 2002. Geochemistry provenance and depositional tectonic setting of the Adigrat Sandstone northern Ethiopia. J. Afr. Earth Sci. 35, 185–198.

Hautot, S., Tarits, P., Whaler, K., Le Gall, B., Tiercelin, J.J, Le Turdu, C., 2000. The deep structure of the Baringo Rift basin (central Kenya) from 3-D magneto-telluric imaging: Implications for rift evolution. J. Geophys. Res. 105, 23493–23518.

Hautot, S., Tarits, P., Perrier, F., Tarits, C., Trique, M., 2002. Groundwater electromagnetic imaging in complex geological and topographical regions: a case study of a tectonic boundary in the French Alps. Geophysics 67, 1048–1060.

Hofmann, C., Courtillot, V., Feraud, G., Rochette, P., Yirgu, G., Ketefo, E., Pik, R., 1997. Timing of the Ethiopian flood basalt event and implications for plume birth and global change. Nature 389, 838–841.

Jepsen, D.H., Athearn, M.J., 1961. A general geological map of the Blue Nile River basin. Ethiopia (1:1.000.000). Department of Water Resources, Addis Ababa.

Jones, A., 1988. Static shift of magnetotelluric data and its removal in a sedimentary basin environment. Geophysics 53, 967–978.

Kappelman, J., Rasmussen, D.T., Sanders, W.J., Feseha, M., Bown, T.M., Copeland, P., Crabaugh, J., Fleagle, J.G., Glantz, M., Gordon, A., Jacobs, B.F., Maga, M., Muldoon, K., Pan, A., Pyne, L., Richmond, B., Ryan, T.J., Seiffert, E.R., Sen, S., Todd, L., Wiemann, M.C., Winkler, A., 2003. New Oligocene mammals from Ethiopia and the pattern and timing of faunal exchange between Afro-Arabia and Eurasia. Nature 426, 549–552.

Kidane, T., Abebe, B., Courtillot, V., Herrero, E., 2002. New paleomagnetic result from the Ethiopian flood basalts in the Abbay (Blue Nile) and Kessem gorges. Earth Planet. Sci. Lett. 203, 353–367.

Kieffer, B., Arndt, N., Lapierre, H., Bastien, F., Bosch, D., Pecher, A., Yirgu, G., Ayalew, D., Weis, D., Jerram, D.A., Keller, F., Meugniot, C., 2004. Flood and shield basalts from Ethiopia: Magmas from the African Superswell. J. Pet. 45, 793–834.

Mège, D., Korme, T., 2004. Dyke swarm emplacement in the Ethiopian Large Igneous Province: not only a matter of stress. J. Volcanol. Geotherm. Res. 132, 283–310.

Morley, C.K., Bosworth, W., Day, R.A., Lauck, R., Bosher, R., Stone, D.M., Wigger, S.T., Wescott, W.A., Haun, D., Basset, N., 1999. Geology and geophysics of the Anza graben. In: Morley, C.K. (Ed.). Geosciences of rift systems. Evolution of East Africa: AAPG study in Geology, 44, 67–90.

Pik, R., Deniel, C., Coulon, C., Yirgu, G., Hofmann, C., Ayalew, D., 1998. The northwestern Ethiopian Plateau flood basalts: classification and spatial distribution of magma types. J. Volcanol. Geotherm. Res. 81, 91–111.

Pik, R., Marty, B., Carignan, J., Lavé, J., 2003. Stability of the Upper Nile drainage network (Ethiopia) deduced from (U–Th)/He thermochronometry: implications for uplift and erosion of the Afar plume dome. Earth Planet. Sci. Lett. 215, 73–88.

Ritter, O., Junge, A., Dawes, G.J.K., 1998. New equipment and processing for magnetotelluric remote reference observations. Geophys. J. Int. 132, 535–548.

Tadesse, S., Milesi, J.-P., Deschamps, Y., 2003. Geology and mineral potential of Ethiopia: a note on geology and mineral map of Ethiopia. J. Afr. Earth Sci. 36, 273–313.

Whaler, K.A., Hautot, S., 2006. The electrical resistivity structure of the crust beneath the northern Ethiopian rift. In: Yirgu, G., Ebinger, C., Maguire, P. (Eds.), Structure and Evolution of the East African Rift in Afar Volcanic Province. Geol. Soc. Spec. Publ., in press.

Wolela, A., 1997. Sedimentology, diagenesis and hydrocarbon potential sandstones in hydrocarbon prospective Mesozoic rift basins (Ethiopia, UK, USA), Ph.D. Thesis, Queen's University of Belfast.

Worku, T., Askin, T.R., 1992. The Karoo sediments (Late Palaeozoic to Early Jurassic) of the Ogaden Basin, Ethiopia. Sediment. Geol. 76, 7–21.